LWT - Food Science and Technology 222 (2025) 117646

Contents lists available at ScienceDirect

LWT

journal homepage: www.elsevier.com/locate/lwt

Origanum majorana essential oil-enriched collagen/K-carrageenan films with enhanced thermal, hydrophobic, anti-oxidant and anti-microbial properties for active Packaging

Saurabh Bhatia [a,b,*,1], Muhammad Jawad [a,1], Sampath Chinnam [c], Ahmed Al-Harrasi [a,**], Yasir Abbas Shah [a], Talha Shireen Khan [a], Esra Koca [d], Levent Yurdaer Aydemir [d], Sevgin Dıblan [e], Dinu Thomas Thekkuden [f], Fahad M. Alshabrmi [g], Md Khalid Anwer [h]

[a] *Natural and Medical Sciences Research Center, University of Nizwa, P.O. Box 33, Birkat Al Mauz, Nizwa, 616, Oman*
[b] *School of Health Science, University of Petroleum and Energy Studies, Dehradun, 248007, India*
[c] *Department of Chemistry, M.S. Ramaiah Institute of Technology, MSR Nagar, Bengaluru, 560054, Karnataka, India*
[d] *Department of Food Engineering, Adana Alparslan Turkes Science and Technology University, 01250, Adana, Turkey*
[e] *Food Processing Department, Vocational School of Technical Sciences at Mersin Tarsus Organized Industrial Zone, Tarsus University, 33100, Tarsus/Mersin, Türkiye*
[f] *Mechanical and Industrial Engineering Department, Abu Dhabi University, 59911, Abu Dhabi, United Arab Emirates*
[g] *Department of Medical Laboratories, College of Applied Medical Sciences, Qassim University, Buraydah, 51452, Saudi Arabia*
[h] *Department of Pharmaceutics, College of Pharmacy, Prince Sattam Bin Abdulaziz University, Al-kharj, 11942, Saudi Arabia*

ARTICLE INFO

Keywords:
Food packaging
Biopolymer
Essential oil
Anti-microbial
Anti-oxidant

ABSTRACT

This research focused on the development of collagen/k-carrageenan based films loaded with Marjoram essential oil (MEO) for active food packaging. Key findings highlighted that elevating MEO concentrations (0.1–1 %) resulted in a notable reduction in the tensile strength (20.41 ± 0.55 to 7.25 ± 0.53 MPa), swelling index (798 ± 9 to 638 ± 25 %), and moisture content (23.50 ± 0.31 to 19.13 ± 0.86 %) of the films while simultaneously increasing the elasticity (11.11 ± 1.69 to 51.21 ± 2.80 %) and water vapor permeability from 0.206 ± 0.008 to 0.507 ± 0.013 (g*mm)/(m^2*h*kPa). The DPPH radical inhibition activity of films increased from 21.03 % to 52.53 %, while the ABTS cation radical inhibition activity rose from 42.90 % to 68.29 % with the addition of MEO. Furthermore, anti-microbial assays showed significant efficacy of films loaded with highest concentration of MEO against common food-borne pathogens including *P. aeruginosa* and *C. albicans*. In addition, the water contact angle measurement analyses revealed that the inclusion of MEO contributed to an increase in the hydrophobicity of the films. Moreover, thermal analysis also revealed the improved thermal stability of the films with the addition of MEO. These findings demonstrate the potential of MEO-loaded films as a potential active packaging material, offering a biodegradable and eco-friendly solution to address the limitations of conventional plastics.

1. Introduction

In food packaging industries, traditional plastic films are extensively used for packaging applications (Dong et al., 2018; Soysal et al., 2015). However, there are several challenges associated with the use of plastic films such as non-biodegradability leading to environmental pollution (Raut et al., 2015). To overcome these challenges, an alternative approach could be followed, which is using biopolymers-based composite films. Carrageenan is a linear polysaccharide, which is FDA-approved and it is known for its film-forming properties and good mechanical strength (Udo et al., 2023). It can be easily turned into transparent anti-microbial packaging film with the incorporation of some active compounds (Kim et al., 2008; Prasetyaningrum et al., 2021). The reported tensile strength for the native κ-Carrageenan film is found to be 65.20 MPa (Bhatia et al., 2024). On the other hand, collagen is known for its physicochemical characteristics, hydrophobicity,

* Corresponding author. Natural and Medical Sciences Research Center, University of Nizwa, P.O. Box 33, Birkat Al Mauz, Nizwa, 616, Oman.
** Corresponding author.
E-mail addresses: sbsaurabhbhatia@gmail.com (S. Bhatia), aharrasi@unizwa.edu.om (A. Al-Harrasi).
[1] These authors contributed equally to this work.

https://doi.org/10.1016/j.lwt.2025.117646
Received 28 November 2024; Received in revised form 10 March 2025; Accepted 12 March 2025
Available online 12 March 2025

biodegradability, and non-toxicity in the food industry (Wang et al., 2017). Therefore, developing a novel composite material to overcome the barrier challenges of k-carrageenan films using hydrophobic polymers such as collagen could be a unique approach to developing composite material.

Several active compounds have been incorporated into films to make them active like essential oils (Çakmak et al., 2020), anti-oxidants such as tocopherols (Zhang et al., 2020), anti-microbial agents for example silver nanoparticles (Carbone et al., 2016), bioactive peptides (Najafian, 2023), and natural extracts such as rosemary extract (Kahya et al., 2022). Due to the broad spectrum of anti-microbial and anti-oxidant activities, essential oils are widely used in films as active compounds (El-Mesallamy et al., 2012; Yahaya et al., 2018). *Origanum majorana* essential oil (MEO), commonly known as marjoram essential oil, is a natural extract renowned for its strong anti-oxidant and anti-microbial properties. It is widely used in food preservation and health applications to combat pathogens and oxidative spoilage (Mehanna et al., 2022; Yasar et al., 2022). It has been reported that the incorporation of zinc oxide nanoparticles and *Melissa officinalis* essential oil into chitosan-based films increased tensile strength, reduced water solubility, and improved anti-microbial activity against foodborne bacteria compared to neat chitosan (Sani et al., 2019). Another study investigated the use of lemon and bergamot essential oils in whey protein isolate films. The results demonstrated that not only anti-microbial properties of these films against pathogens such as *Staphylococcus aureus* and *Escherichia coli* were enhanced but also barrier to water vapor permeability and tensile strength also improved [12]. The development and characterization of carrageenan-based films incorporated with essential oils developed for packaging chicken patties showed a bactericidal effect against microorganisms and also exhibited improved physicochemical proprieties (Soni et al., 2016). Therefore, the addition of GRAS-approved natural additives like essential oil in the composite films to improve the anti-oxidant effects could be a more reliable approach.

The widespread use of traditional plastic films in food packaging presents major environmental concerns, including non-biodegradability and pollution, which has encouraged the search for more sustainable alternatives. Previous studies have focused on biopolymer based films, but challenges remain in improving their mechanical strength, water resistance, and anti-microbial efficacy. This study aims to develop collagen/k-carrageenan-based films incorporated with MEO, known for its natural anti-oxidant and anti-microbial properties. The primary objective is to assess the physical, chemical, water vapor barrier, optical, anti-oxidant and anti-microbial properties of these biopolymer based films and to determine their suitability for active food packaging applications.

2. Materials and methods

Biopolymers including collagen (Marine Fish extrapure, 95 %) and kappa-carrageenan (Refind ex.*Eucheuma Cottonii*) were obtained from Sisco Research Laboratories Pvt Ltd., located in Mumbai, India. Marjoram essential oil (Batch no: NNIMAEO/152/0821) was procured from Nature Natural India. Glycerol (anhydrous with a purity of 99.0 %) was purchased from BDH Laboratory Supplies, London, UK.

2.1. Film sample preparation

The film-forming solutions (FFSs) were prepared following the casting method. After the optimization, different film formulations were prepared with various concentrations of MEO as presented in Table 1. The solution of collagen (1.5 % w/v) was prepared using a magnetic stirrer set at a temperature of 40 °C and a stirring speed of 300 rpm for 2 h. Moreover, the solution of k-carrageenan (1.5 % w/v) was also prepared using the same technique by using magnetic stirrer set at a temperature of 60 ± 5 °C and a stirring speed of 400 rpm for 4 h. Glycerol was used at concentration of 0.5 % (v/v) as a plasticizer in each FFS. A 1:1 ratio of the two polymers was used for the preparation of the composite material. MEO and Tween 80 were incorporated into the FFS as per the concentrations specified in Table 1. The FFS (20 ml) was poured into plastic petri plates (90 × 14 mm) and dried in a constant-temperature using drying oven (BOV-T105F, Biobase Bioland Co., Ltd. Jinan, Shandong, China) at 35 ± 2 °C for 48 h. After drying, the film samples were peeled off from the petri dishes and stored at 50 % relative humidity and 25 ± 2 °C for 24 h in climate incubator (BJPX-A400, Biobase Bioland Co., Ltd. Jinan, Shandong, China) ahead of any subsequent tests.

Table 1
Chemical composition of the film forming solutions.

Sample codes	Chemical composition of the film-forming solution
COC1	Collagen (1.5 %) + k-Carrageenan (1.5 %) + Gly (0.5 %)
COC2	Collagen (1.5 %) + k-Carrageenan (1.5 %) + Gly (0.5 %) + MEO (0.1 %) + Tween 80 (0.1 %)
COC3	Collagen (1.5 %) + k-Carrageenan (1.5 %) + Gly (0.5 %) + MEO (0.5 %) + Tween 80 (0.5 %)
COC4	Collagen (1.5 %) + k-Carrageenan (1.5 %) + Gly (0.5 %) + MEO (1 %) + Tween 80 (1 %)

*COC1 (control); COC2 (MEO 0.1 %); COC3 (MEO 0.5 %); COC4 (MEO 1 %).

2.2. Thickness and mechanical attributes

To investigate the impact of MEO on the film samples, the thickness of COC1-COC4 films was measured with a digital micrometer (Yu-Su 150, Yu-Su Tools, Shanghai, China). Thickness evaluations were conducted at ten varied points across each film sample, and the average thickness was calculated in millimeters. The recorded thickness values were subsequently utilized for additional analyses. Additionally, the mechanical characteristics of the COC1-COC4 films were evaluated following the standard method of ASTM (D882) Testing, 2002. A texture analyzer (TA.XT plus, Stable Micro Systems, England) was used for this test at a speed of 30 mm/min. Rectangular strips measuring 60 mm in length and 7 mm in width were securely held between the clamps of a texture analyzer. The tensile strength (TS) and the elongation at break (EAB) were calculated from the Exponent Connect software platform, integrated with the testing machine.

2.3. Water vapor permeability, swelling index and moisture percentage

The assessment of water vapor permeability (WVP) for the film samples was conducted by measuring changes in weight using the method outlined by Gökkaya Erdem et al. (Erdem et al., 2019). These measurements were carried out using glass cups with dimensions of 2 cm in depth and 5 cm in inner diameter. The internal and external relative humidity levels were adjusted using silica gel to achieve 0 % relative humidity (RH) and saturated sodium chloride solution to achieve 100 % RH, all while maintaining a temperature of 25 ± 2°.

The WVP calculation was performed using Equation (1).

$$W = \Delta \boldsymbol{m} / [(\Delta \boldsymbol{t})\ (\Delta \boldsymbol{p})\ (\boldsymbol{A})] \times \boldsymbol{d} \quad (1)$$

- $\Delta m/\Delta t$ signifies the rate at which moisture accumulates expressed in kg/s, A denotes the exposed surface area of the film in m^2, ΔP represents the difference in water vapor pressure across the film in Pa, d corresponds to the thickness of the film in mm.

The swelling index of COC films was assessed following the testing procedure described by Erdem et al. (Erdem et al., 2019). Initially, square film samples ($2 \times 2\ cm^2$) were prepared, and their initial weights (W_1) were recorded. The films were immersed in deionized water at 25 °C for 2 min. After blotting to remove excess water, final weights

(W_2) were measured. The swelling index was calculated using equation (2).

$$\text{Swelling Index} = \frac{W2 - W1}{W1} \times 100 \quad (2)$$

Additionally, the moisture percentage of the COC films was determined using the gravimetric method in which the weight of the films before and after drying was quantified. The films were cut into 30 mm × 40 mm strips, and their initial weight was accurately determined, designated as W1. Afterwards, the films were exposed to controlled drying conditions at 105 °C in until they reached a consistent weight. The weight of the dried films was recorded as W2, and the degree of weight reduction was calculated using Equation (3).

$$MC = \frac{W1 - W2}{W1} \times 100 \quad (3)$$

2.4. Transparency and color attributes

The degree of transparency in the films was evaluated through spectrophotometric analysis using an ONDA-Vis spectrophotometer, following the method established by Erdem et al. (Erdem et al., 2019). To evaluate the color related attributes of the COC1-COC4 films, a spectrophotometer CR-5 (Konica Minolta) was utilized.

2.5. Anti-oxidant capacity of the fabricated films

The radical scavenging activities evaluation of the fabricated films was performed by ABTS cation and DPPH free radical scavenging assays. The COC1-COC4 films were tested for their ABTS free radical scavenging ability as per the methodology outlined by Re et al. (Re et al., 1999). On the other hand, the DPPH assay was carried out following the method described by Brand-Williams et al. (Brand-Williams et al., 1995). For DPPH assay 50 mg of the film sample, for ABTS assay 1.66 mg of the film sample was used. The findings were expressed as % of inhibition.

2.6. Film characterization

The micrographs of the COC1-COC4 films were obtained using a scanning electron microscope (JSM6510LA Analytical Jeol, Tokyo, Japan) with the procedures outlined in a previous study (Bhatia et al., 2023). The films were mounted on aluminum stubs with double-sided tape and coated with gold for improved visibility during imaging.

The chemical interactions within the film matrix were studied using the FTIR Infrared Tensor 37 instrument (InfraRed Bruker, Ettlingen, Germany). The FTIR spectra of the film samples were recorded in the 4000–400 cm^{-1} range. Moreover, the crystalline and amorphous nature of the COC1-COC4 films was assessed using X-ray diffraction analysis performed with a Bruker D8 Discover. The conditions were set at 40 kV, scanning from 5° to 50° in 2θ at 0.5 s per data point, utilizing copper (Kα) radiation at a wavelength of 1.5418 Å. Furthermore, thermal analysis data including thermogravimetric analysis (TGA), differential scanning calorimetry (DSC), and derivative thermogravimetry (DTG) were obtained by employing a TA (model SDTQ600, TA Instruments New Castle, Delaware, USA). A 10 mg sample of the film was sealed in an airtight aluminum capsule and heated from 25 °C to 600 °C at 10 °C per minute under a nitrogen-rich atmosphere.

2.7. Anti-microbial activity of the fabricated films

The anti-microbial activity of films COC1-COC4 was assessed using a modified agar diffusion method, as described by Seol et al. (Seol et al., 2009) and Matuschek et al. (Matuschek et al., 2014). For this study, *Candida albicans* (Fungi) and *Pseudomonas aeruginosa* (a Gram-negative bacterium) were selected. Prior to the study, all microorganisms were activated using Tryptic soy agar (TSA) by incubating at 35 °C for 18 h. Film discs of 1 cm were placed on Mueller–Hinton agar inoculated with *Candida albicans* and *Pseudomonas aeruginosa* were subjected to incubation at 35 °C for 24–48 h. Inhibition zones, which appeared as clear areas surrounding the film discs, were measured in millimeters across the discs.

2.8. Contact angle measurements

The surface properties of the COC1-COC4 films loaded with and without MEO were analyzed using a goniometer (OCA11 Data Physics Instruments GmbH, Filderstadt, Germany). A syringe loaded with water was placed in a syringe holder. COC sample films (2 × 2 cm) were cut and placed on the sample platform. A drop of distilled water was dropped on the COC film surface, and the CA was assessed by using dpiMAX software. OCA11 camera with a resolution of 1044 × 1080 was employed to take images of the water droplet.

2.9. Statistical analysis

The results acquired in this study were expressed as the mean value with its associated standard deviation (SD) from a set of three replicates. A one-way analysis of variance (ANOVA) with post hoc Duncan's test was applied using SPSS Inc. in Chicago, IL, USA.

3. Results and discussion

3.1. Thickness and mechanical attributes

Table 2 provides the thickness data of the formulated films. The values of thickness for COC1-COC4 ranged between 0.026 ± 0.005 to 0.056 ± 0.005 mm. The thicknesses of the oil-loaded films did not change significantly; however, the blank film COC1 had a lower thickness value (0.026 mm). The initial increase in thickness may have been caused by the addition of MEO, which increased the dry matter content in the matrix (Lee et al., 2019). Other studies have also observed similar findings (Gahruie et al., 2017; Ghani et al., 2018; Song et al., 2018). The findings contradicted some earlier studies that suggested a direct correlation between essential oil content and film thickness (Atef et al., 2015; Simsek et al., 2020).

The effect of various concentrations of MEO on the mechanical properties of COC1-COC4 composite films is presented in Table 4. Composite films without oil showed TS 20.41 ± 0.55 MPa, which is less than the reported TS value (26.291 MPa) of kappa carrageenan native films (Park, 1996; Shojaee-Aliabadi et al., 2014). This variation could be due to the variation in the amount of FFS poured or processing conditions of the films. Additionally, as the concentration of oil increased, the fabricated films' tensile strength decreased while their EAB values dramatically increased ($p < 0.05$), resulting in softer and more flexible films (Arfat et al., 2014; Shen & Kamdem, 2015; Sun et al., 2020). The drop in TS could be due to the decrease in the intra- and inter-molecular interactions with the increase in the concentration of oil. Moreover, the plasticization behavior of oil may be the cause of an increase in EAB values with a rise in MEO proportion, as this could improve the flexibility and polymer chain mobility in the film. These results align with

Table 2
Thickness and mechanical properties of control and MEO incorporated COC films.

Sample Code	Thickness (mm)	TS (MPa)	EAB (%)
COC1	0.026 ± 0.005[a]	20.41 ± 0.55[a]	11.11 ± 1.69[a]
COC2	0.052 ± 0.008[b]	12.71 ± 0.61[b]	30.17 ± 1.63[b]
COC3	0.054 ± 0.009[b]	9.60 ± 0.51[c]	42.46 ± 2.25[c]
COC4	0.056 ± 0.005[b]	7.25 ± 0.53[d]	51.21 ± 2.80[d]

*COC1 (control); COC2 (MEO 0.1%); COC3 (MEO 0.5%); COC4 (MEO 1%). The difference between the mean values ($p < 0.05$) is represented by the letters[a-d].

Table 3
Water vapor permeability (WVP), swelling index (SI), and moisture content (MC) of control and MEO-incorporated COC films.

Sample Codes	WVP ((g[a]mm)/(m2[a]h[a]kPa))	Swelling index (%)	Moisture content (%)
COC1	0.206 ± 0.008[a]	798 ±9[a]	23.50 ± 0.31[a]
COC2	0.372 ± 0.010[b]	731 ± 25[b]	23.36 ± 0.70[a]
COC3	0.423 ± 0.022[c]	693 ± 24[bc]	20.99 ± 0.42[b]
COC4	0.507 ± 0.013[d]	638 ± 25[c]	19.13 ± 0.86[c]

[a] COC1 (control); COC2 (MEO 0.1 %); COC3 (MEO 0.5 %); COC4 (MEO 1 %). The difference between the mean values ($p < 0.05$) is represented by the letters [a-d].

the findings of the earlier research (Kavoosi et al., 2014; Zhou et al., 2021).

3.2. Water vapor barrier, swelling index, and moisture content analysis

WVP of films ranged between 0.206 ± 0.008 and 0.507 ± 0.013 (g*mm)/(m2*h*kPa) (Table 3). The WVP of the control film was 0.206 ± 0.008 (g*mm)/(m2*h*kPa). As the MEO concentration increased, WVP levels also increased. According to earlier research, this might be the result of the development of the free space in the film structure, which increases molecular mobility (Ghasemlou et al., 2013; Simsek et al., 2020). The increase in free volume could be attributed to the increase in the concentration of MEO. Similar findings were also concluded in the earlier studies where high concentrations of oil create deformities in the form of cracks, pores, or fractures in the films, facilitating the passage of more moisture across the films (Atef et al., 2015; Jouki et al., 2014). It has also been concluded in previous studies that various factors influence the water vapor permeability of films, including the balance between hydrophobic and hydrophilic groups, the presence of cracks, the level of porosity, and the complexity of the film's internal pathways (Jahed et al., 2017). This suggests that essential oils or other hydrophobic compounds do not always enhance the water vapor barrier of polymer-based films.

The swelling index (SI) of COC-based edible film is presented in Table 2. SI of the prepared films ranged between 798 ± 9 and 638 ± 25. The swelling index of the films was considerably ($p < 0.05$) reduced with the addition of MEO in a concentration-dependent manner, indicating that the hydrophobicity of the films increased as the amount of MEO in the films increased. This finding suggests that higher concentrations of MEO make the films less prone to swelling by water and this behaviour could be associated with the hydrophobic nature of the oil. The essential oils' hydrophobic components interact with the polymer matrix, reducing the film's affinity for water (Hasheminya et al., 2019). These results are consistent with earlier studies that reported that introducing essential oil decreased the SI of the resulting films (Hopkins et al., 2015; Xue et al., 2019).

For films to perform well and be suitable as a material for food packing, analyzing their moisture percentage is essential. According to Table 2, the MC values decreased as the amount of the MEO increased in the COC films. The control film showed 23.50 ± 0.31 % moisture, which significantly ($p < 0.05$) decreased to 19.13 ± 0.86 % in the COC4-coded films. This shows the highest MC value in the control film, while the lowest values in COC3 and COC4 coded films. The decrease in MC values may be explained by the addition of hydrophobic agents (MEO) to the films, which causes an interaction between the EO components and the hydroxyl groups of the polymer matrix. The findings were consistent with earlier research (Dashipour et al., 2015; Simsek et al., 2020).

Table 4
Optical properties of blank and MEO incorporated COC films. COC1 (control); COC2 (MEO 0.1 %); COC3 (MEO 0.5 %); COC4 (MEO 1 %).

Sample Code	L	a[a]	b[a]	Opacity
COC1	95.70 ± 0.28[a]	−0.15 ± 0.01[a]	1.11 ± 0.10[a]	1.19 ± 0.17[a]
COC2	95.75 ± 0.02[a]	−0.13 ± 0.00[a]	1.00 ± 0.02[a]	1.05 ± 0.08[a]
COC3	96.14 ± 0.03[b]	−0.08 ± 0.04[b]	1.00 ± 0.05[a]	1.03 ± 0.14[a]
COC4	97.67 ± 0.34[c]	0.07 ± 0.07[c]	1.03 ± 0.02[a]	0.97 ± 0.09[a]

[a] COC1 (control); COC2 (MEO 0.1 %); COC3 (MEO 0.5 %); COC4 (MEO 1 %). The difference between the mean values ($p < 0.05$) is represented by the letters [a-d].

3.3. Optical properties of the film

It is usually recognized that food packaging with an opacity of less than five is considered transparent (Lei et al., 2021). For food packaging materials, the acceptable limit value of transparent materials is around 80 % transmittance (Lei et al., 2021). In the current investigations, the opacity of the films ranged between 1.19 ± 0.17 to 0.97 ± 0.09, as presented in Table 4. The opacity of the composite films slightly decreased with the increase in the concentration of MEO. The decrease of the opacity due to MEO addition could be because of the influence of the additive on the film plasticization. A previous study reported similar results where the addition of surfactant was reported to reduce the polymeric interactions, which resulted in a decrease in film opacity (Carneiro-da-Cunha et al., 2009).

Color evaluation of the films is a crucial factor that determines consumer acceptability of packaging materials. Optical attributes of the films are often dependent on the type of additives utilized in their preparation (Arrieta et al., 2014). The differences in color of all composite films are presented in Table 3. The yellowishness (expressed as the b* value) among the films showed a slight variation with the increase in the concentration of oil, as shown in Table 3. This finding was in agreement with the previous research where the addition of *Mentha pulegium* essential oil in the films did not cause significant differences in L, a*, and b* values (Simsek et al., 2020). Furthermore, samples COC1 and COC2 showed no apparent differences ($P < 0.05$) in lightness (L value), a* values, and yellowishness (expressed as the b* value) among the films.

3.4. Anti-oxidant assays (DPPH and ABTS)

Edible films loaded with essential oils or plant extracts demonstrate favorable anti-oxidant effects and are considered as good alternative to synthetic anti-oxidants. Figs. 1 and 2 represent the anti-oxidant properties of the films with increasing the concentration of MEO. The anti-oxidant activities of the prepared films were assessed by using DPPH and ABTS assays. The results of this investigation show that when MEO is added to the films, their ability to scavenge radicals such as DPPH and ABTS cation increased. While the control sample exhibited the lowest level of anti-oxidant activity, the COC4 film sample with the highest concentration of MEO demonstrated the highest levels of DPPH and ABTS cation radical scavenging ability. After adding MEO, the film samples' DPPH and ABTS cation radical scavenging activity increased, rising from 21.03 to 52.53 % and from 42.9 to 68.29 %, respectively. These results indicated that the anti-radical activity of the composite film was significantly ($p < 0.05$) increased as the MEO content increased.

The presence of the phenolic compounds in the MEO may be responsible for the increased anti-oxidant activity of the films (Paudel et al., 2022; Schmidt et al., 2008). Similar results were also observed in the previous investigations, where anti-oxidant capacity increased with an increase in the concentration of oil (Tongnuanchan et al., 2013, 2014). Such active packaging material could be used commercially to pack food products that are highly vulnerable to oxidation.

3.5. The microstructural properties of films

The surface and cross-sectional micrographs of the prepared films are presented in Fig. 3. The surface micrograph of the blank films displayed

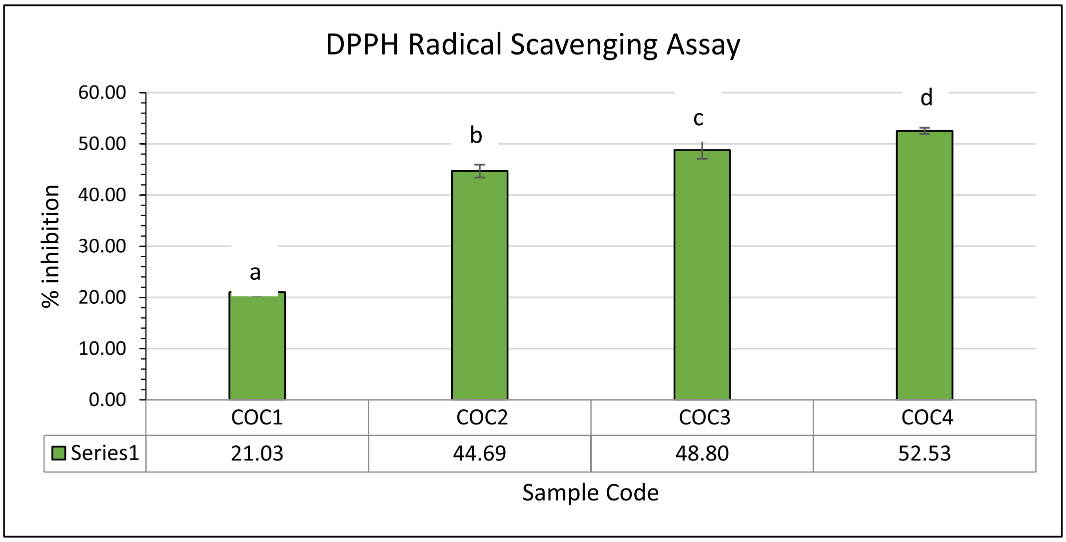

Fig. 1. DPPH radical scavenging assay of COC films formulated with and without different concentrations of marjoram essential oil (MEO). COC1 (control); COC2 (MEO 0.1 %); COC3 (MEO 0.5 %); COC4 (MEO 1 %). The difference between the mean values ($p < 0.05$) is represented by the letters [a-d].

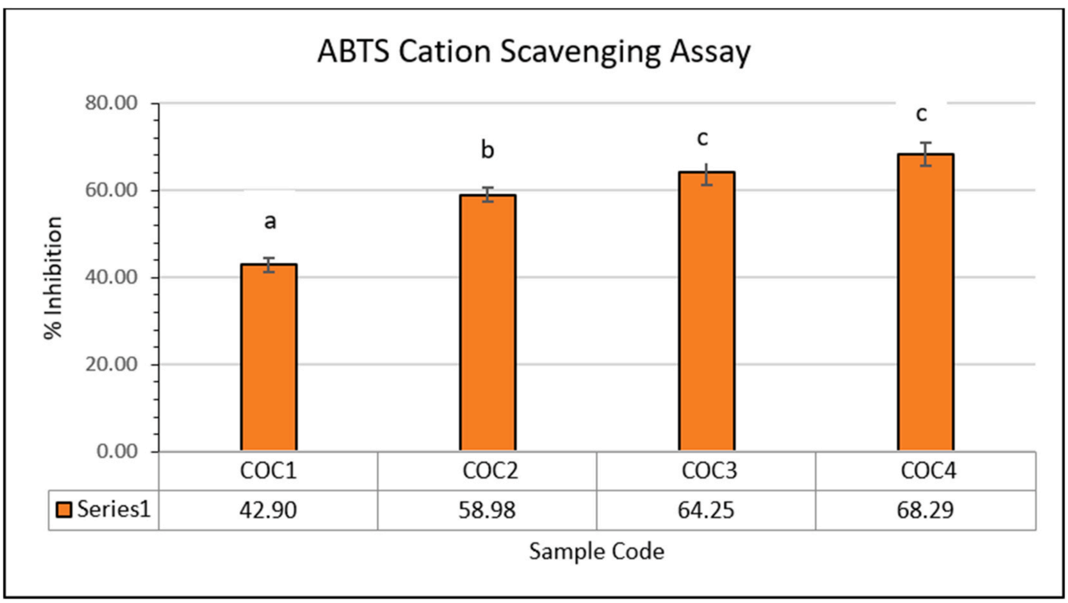

Fig. 2. ABTS cation radical scavenging assay of COC films formulated with and without different concentrations of marjoram essential oil (MEO). COC1 (control); COC2 (MEO 0.1 %); COC3 (MEO 0.5 %); COC4 (MEO 1 %). The difference between the mean values ($p < 0.05$) is represented by the letters [a-d].

smooth and continuous microstructure with the appearance of only a few particles. These findings are in accordance with a previous study, where pure κ-carrageenan film demonstrated smooth and continuous microstructure, suggesting the compatibility between collagen and κ-carrageenan (Shojaee-Aliabadi et al., 2013). Their cross-sections of all films showed a fine and uniform texture with insignificant changes. It was found that the surface roughness and agglomeration increased with the increase in the MEO concentration. This could be associated with the presence of MEO, which reduces polymer interaction in the film network. This finding is in accordance with the previous study (Liu et al., 2021). The microstructure of COC2 films with lower concentrations of MEO was almost similar to that of blank film, as droplets of the oil were well incorporated into the polymer matrix (Bonilla et al., 2012), while the films loaded with a higher proportion of MEO showed more roughness and visible agglomeration because of the rise of the collision frequency among droplets in oil-in-water solutions (Ghasemlou et al., 2013). Furthermore, because of the slight flocculation, creaming, and coalescence of substances that took place in the membrane liquid, the film displayed more irregular and uneven surface features as the size and quantity of droplets increased (Song et al., 2018).

3.6. FTIR

To understand the interaction between the functional groups of various components, the FTIR analysis is performed (Moni et al., 2021). The FTIR spectra of collagen/k-carrageenan films are presented in Fig. 4. A wide band observed in the range of 3000–3500 cm^{-1} could be linked to the amide A stretching (N-H stretching) found in collagen and the –OH stretching, which is a distinctive vibration of carrageenan. Furthermore, the spectra consistently display absorption bands that are specific to collagen's peptide bonds, i.e., C=O stretching of amide I at 1633 cm^{-1}, N-H bending of amide II at 1546 cm^{-1}, and C-N stretching of amide III at 1218 cm^{-1} (Andonegi, Irastorza, et al., 2020). The fingerprint region between 1200 cm^{-1} and 900 cm^{-1} can be associated with

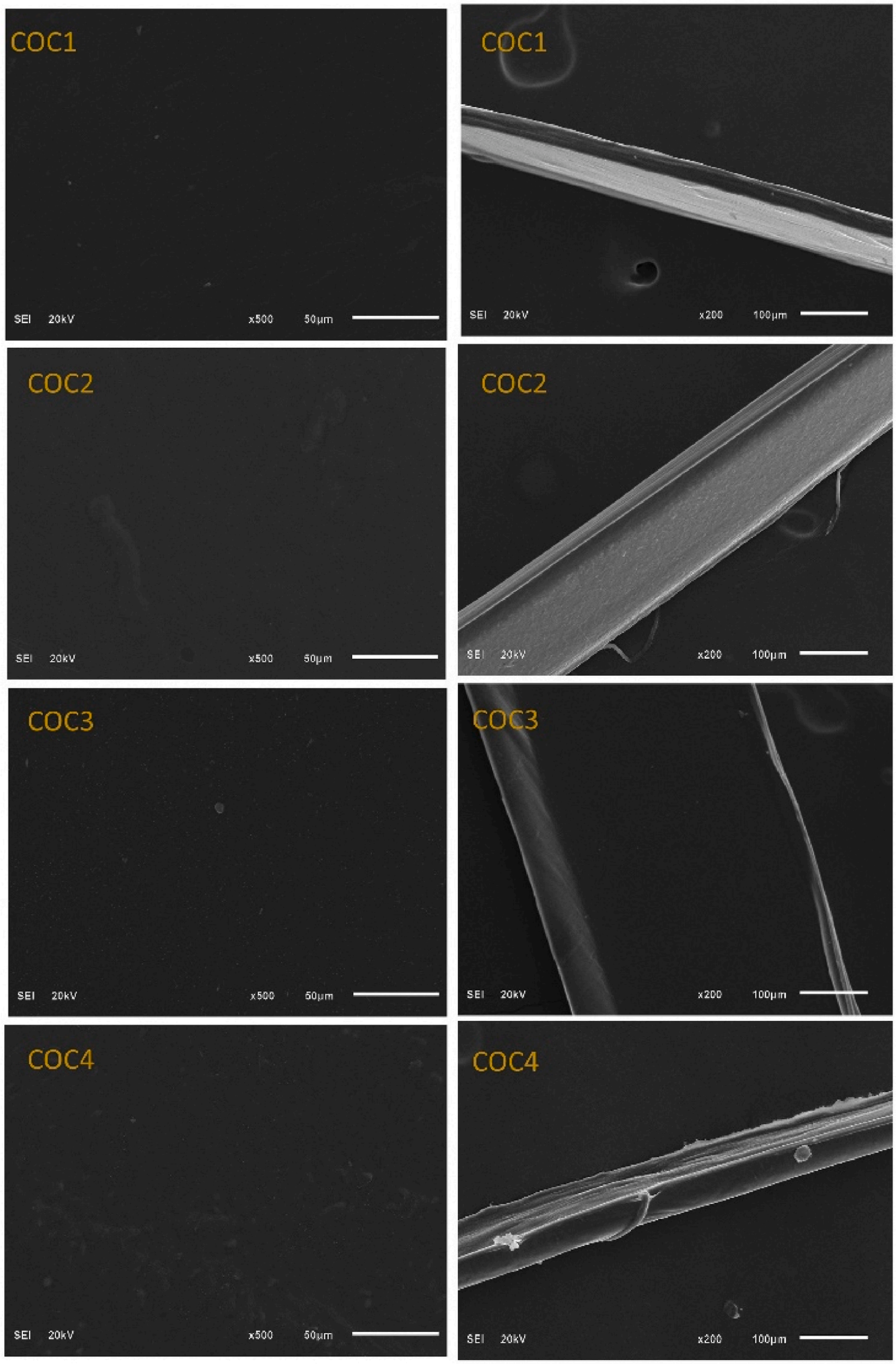

Fig. 3. SEM micrographs of COC films formulated with and without different concentrations of marjoram essential oil (MEO). COC1 (control); COC2 (MEO 0.1 %); COC3 (MEO 0.5 %); COC4 (MEO 1 %).

the C-O bond stretching vibrations in collagen and those of hydroxyl groups present in glycerol (Andonegi, de la Caba, & Guerrero, 2020).

In addition, functional group related to k-carrageenan were identified across the entire examined spectral range. The asymmetric and symmetric stretching vibrations of the C–H bonds in the methylene groups of carrageenan are evident at the spectral range 2925 and 2875 cm^{-1}. In the spectral region spanning from 900 to 1200 cm^{-1}, the vibration patterns of oxygen-containing groups present in carrageenan were observed. The stretching of C–O in 3,6-anhydro-D-galactose was observed around 918 cm^{-1}, at 1033 for C–O groups along with glycosidic linkage, and asymmetric stretching of C–O–C at 1158 cm^{-1}. Furthermore, vibrations related to sulfate groups in carrageenan are predominantly noted at 840 cm^{-1} (D-galactose-4-sulfate), 1218 cm^{-1} (sulfate ester asymmetric stretching), and 1340 cm^{-1} (sulfate stretching). Each spectral peak observed in the current study was assigned as per the literature (Ortiz-Tafoya & Tecante, 2018; Simona et al., 2021). Overall, the chemical interaction between the biopolymers and the MEO was observed in the FTIR spectrum.

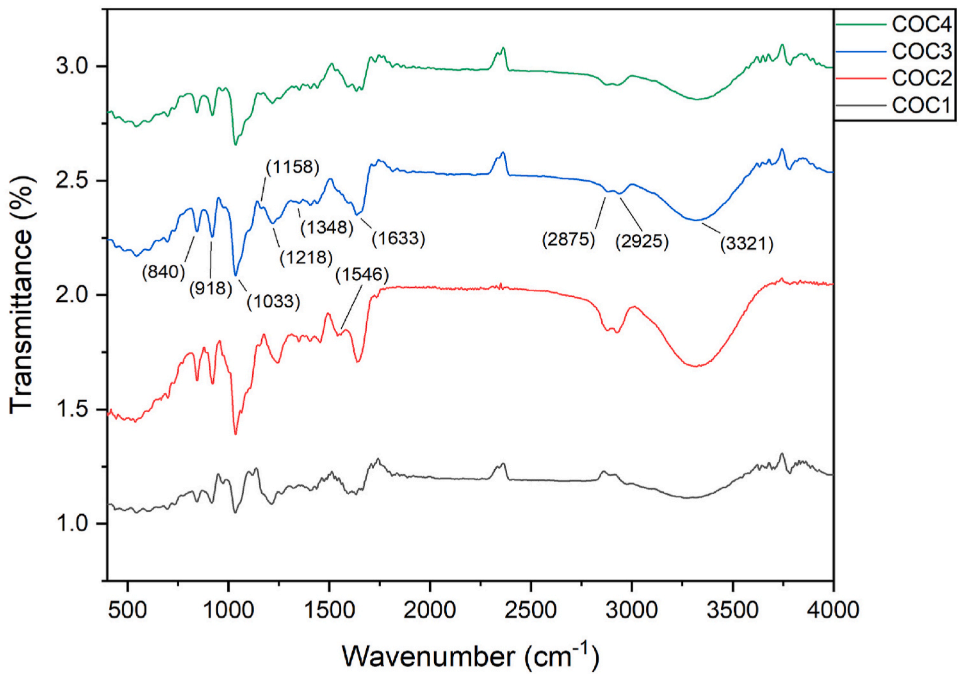

Fig. 4. FTIR analysis of COC films formulated with and without different concentrations of marjoram essential oil (MEO). COC1 (control); COC2 (MEO 0.1 %); COC3 (MEO 0.5 %); COC4 (MEO 1 %).

3.7. X-ray diffraction (XRD) analysis

XRD spectra of the collagen/k-carrageenan films with and without MEO are shown in Fig. 5. All composite films showed diffraction peaks at about 7.8° (sharp), 20.5° (wide), and 31° (sharp), which were in accordance with the characteristic diffraction peaks of collagen (Ata et al., 2024; Giraud-Guille et al., 2000; Rezaei et al., 2021; Vedhanayagam et al., 2020). The first and second peaks formed at 2θ from 20° to 31° could be attributed to the κ-carrageenan-based film as reported in earlier research. Also, the peak formed at 2θ = 31° could be due to the

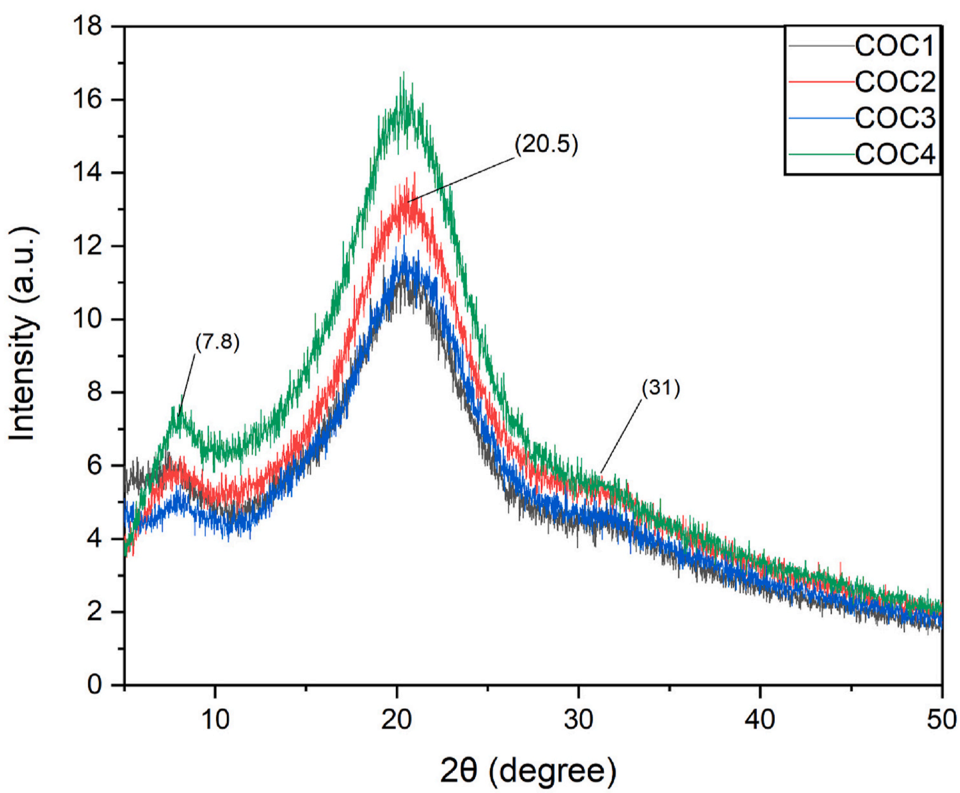

Fig. 5. XRD of COC films formulated with and without different concentration of marjoram essential oil (MEO). COC1 (control); COC2 (MEO 0.1 %); COC3 (MEO 0.5 %); COC4 (MEO 1 %).

presence of a small amount of salt crystallites in collagen samples (Adam et al., 2020; Azizi et al., 2017; Rezaei et al., 2021). Additionally, the peak that appeared at around $2\theta = 31^{\circ}$ is probably the result of inorganic salts like potassium chloride that are present in the films of κ-carrageenan (Martins et al., 2012). It was found that with the increase in the concentration of oil, peak intensities decreased, and overall crystallinity also decreased, as shown in Fig. 4. The decrease in peak intensities after the addition of MEO could be due to the decrease in hydrogen bonding, resulting in a decrease in regular domains, compactness, and film crystallinity. This is mainly due to the plasticization effect of oil after its incorporation into the films, resulting in an increase in the amorphous regions of the films' structure (S. G.-G. Aziz & Almasi, 2018; Aziz et al., 2018) These findings were in accordance with mechanical assessment results, in which the addition of oil resulted in a decrease in tensile strength while EAB value increased as mentioned in Table 2 (Salama et al., 2019). The crystallinity of the present films ranged between 30.5 and 40.3 %, which was comparatively higher than the crystallinity of the LDPE films (37.8 %) as reported in the previous study (Sakdapipanich et al., 2022).

3.8. Thermal properties

The effect of MEO concentration on the thermal stability of the films was analyzed using TGA, DTG, and DSC. The weight loss (TG curves), rate of change of mass with respect to temperature (DTG curves), and thermal transformation (DSC curves) are presented in Fig. 6 (a) and 6 (b), and 6 (c), respectively. The weight loss in the films took place at four major stages, as detected in Fig. 6 (a) and 6 (b). The first weight loss between 30 and 150 °C designated as T1, could be due to the loss of free or bound water in the films (Kchaou et al., 2020; Yekta et al., 2020)

It was found that the COC2 sample showed less weight loss in comparison to other samples. However, the weight loss observed among all samples at a temperature of 150 °C is almost the same. The second weight loss, T2 (160–300 °C), could be due to the volatilization of aldehydes, Tween 80, and glycerol in the film. Third (T3: 310–350 °C) and fourth (T4: 360–450 °C) weight losses could be due to degradation or decomposition of polymers between 310 and 450 °C. As shown in TGA and DTG graphs, the EO-containing films showed less thermal decomposition than the control in between 160 and 420 °C, indicating better thermal stability (Gheribi et al., 2018; Xue et al., 2019)

Variations in endothermic peak temperature with the inclusion of oil can be observed in Fig. 6 (c). This indicates the EO component and the polymer matrix have a significant molecular interaction. The lower residual moisture content in the MEO-containing film (compared to the control) may be the cause of the greater Tg in the matrix. These results were consistent with earlier research (Gheribi et al., 2018). Because the films containing EO showed greater Tg values than the control, this suggests that the glass-to-rubber transition (or vice versa) happens in these films at higher temperatures, indicating improved thermal stability (Xue et al., 2019). The increase in thermal stability could be due to several phenol and aldehyde substances in MEO exhibiting extremely high thermal stability (Kang & Song, 2019).

TGA, DTG, and DSC analyses showed that incorporation of MEO not only enhances the thermal property but also might expand application in practical environments, where higher thermal stability is required.

3.9. Anti-microbial assay

The anti-microbial activities of MEO-loaded COC films were examined against *Pseudomonas aeruginosa* and *Candida albicans*. The findings for the anti-microbial capacity of the films are given in Table 5. The COC samples incorporated with MEO showed good anti-microbial activity. Zone of Inhibition (ZOI) was not observed in COC1 control films in comparison to the essential oil-loaded films. COC4 films (maximum concentration of MEO) showed a clear ZOI of 28.41 mm (*P. aeruginosa*) and 29.99 mm (*C. albicans*). The results clearly show that the anti-microbial effect of COC films is due to the incorporation of MEO in the film matrix.

The anti-microbial effects of MEO have been extensively reported in previous studies against various microorganisms. The essential oils contain monoterpenes such as α-terpineol, α-pinene, and *p*-cymene, which are mainly responsible for the anti-microbial activities of the EOs

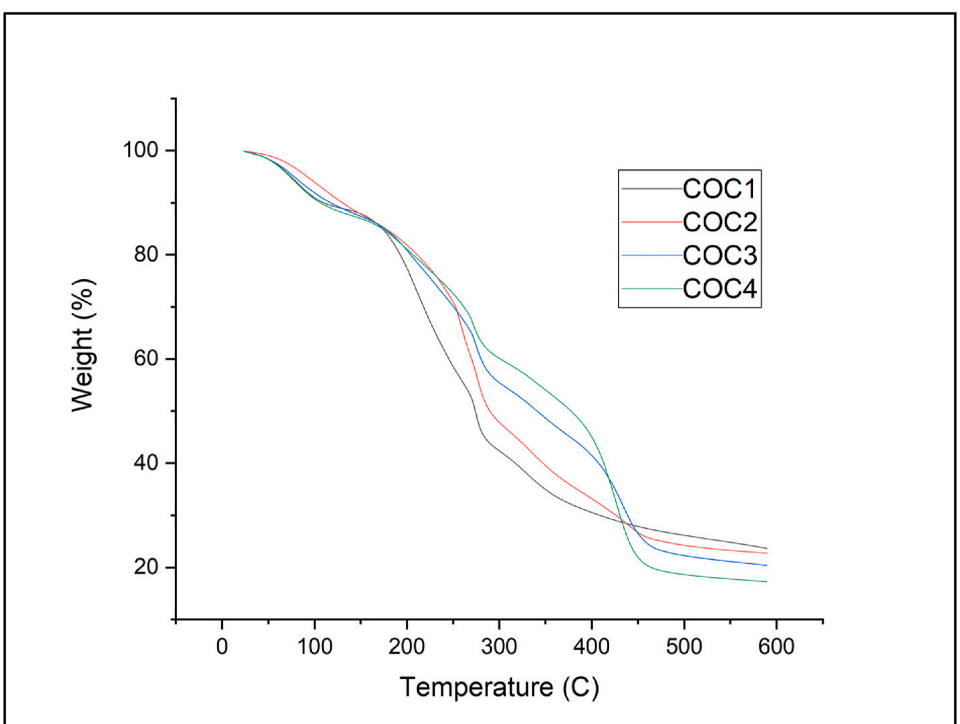

Fig. 6 (a). TGA of blank and MEO incorporated COC films. COC1 (control); COC2 (MEO 0.1 %); COC3 (MEO 0.5 %); COC4 (MEO 1 %).

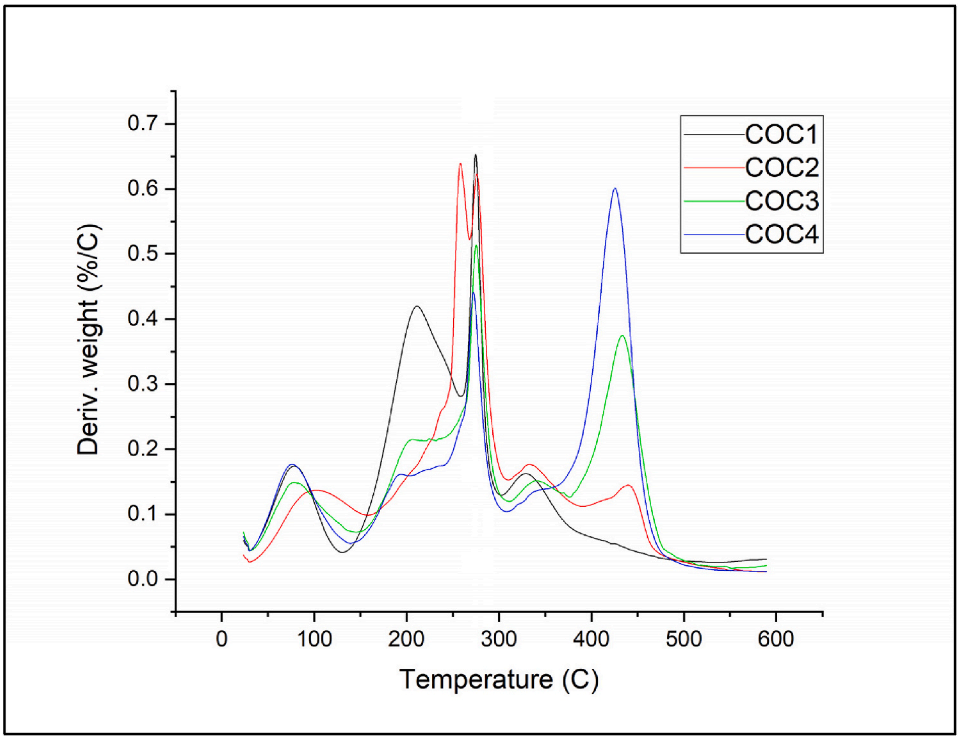

Fig. 6 (b). DTA of blank and MEO incorporated COC films. COC1 (control); COC2 (MEO 0.1 %); COC3 (MEO 0.5 %); COC4 (MEO 1 %).

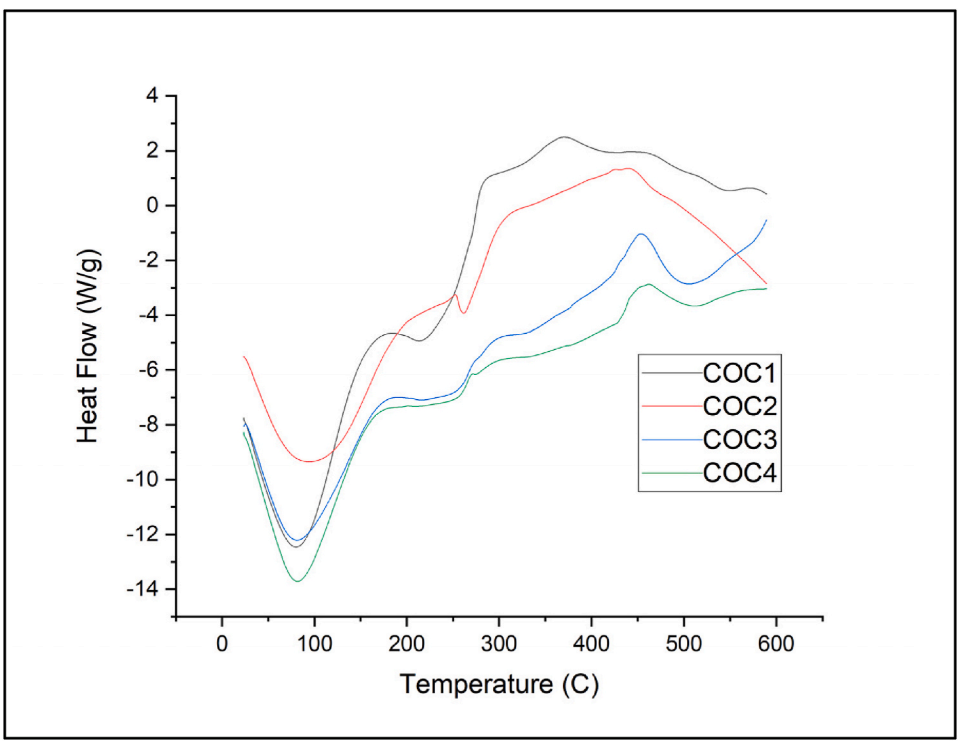

Fig. 6 (c). DSC of blank and MEO incorporated COC films. COC1 (control); COC2 (MEO 0.1 %); COC3 (MEO 0.5 %); COC4 (MEO 1 %).

(Cimanga et al., 2002; Paudel et al., 2022). Therefore, antimicrobial activity could be due to the incorporation of MEO and its various constituents present in the EO. The findings (Fig. 7) suggest that MEO has the potential to function as a natural preservative in polymeric films against foodborne pathogens, including *P. aeruginosa* and *C. albicans*. A previous study conducted by Negar et al. (Haghighatpanah et al., 2022) on mung bean protein and pullulan-based films reported similar anti-microbial results due to the incorporation of MEO in the polymeric films. Overall, these findings highlight the potential of MEO-loaded COC films as effective natural preservatives in food packaging, offering an eco-friendly alternative to synthetic additives and contributing to improved food safety and shelf life.

Table 5
Anti-microbial assay of blank and MEO incorporated COC films.

Sample Codes	Zone of Inhibition (mm)	
	P. aeruginosa	C. albicans
COC1	No Zone	No Zone
COC2	17.46 ± 2.45^a	28.26 ± 1.43^a
COC3	24.70 ± 3.14^b	26.30 ± 2.87^b
COC4	28.41 ± 3.59^c	29.99 ± 8.60^c

*COC1 (control); COC2 (MEO 0.1%); COC3 (MEO 0.5%); COC4 (MEO 1%). The difference between the mean values ($p < 0.05$) is represented by the letters $^{a\text{-}d}$.

3.10. Surface properties

Contact angle measurement helps in determining the hydrophobicity or hydrophilicity of material surfaces. Fig. 8 presents the water contact angle of the films with and without oil. The blank film showed the lowest water contact angle value among all film samples. As the oil concentration increased from 0.5 to 1 %, the water contact angle of the film surfaces increased significantly ($P \leq 0.05$). The hydrophobic essential oil addition to the hydrophilic film materials caused this change in the surface behavior, which led to a decrease in the hydrophilicity of oil-loaded films as the MEO amount increased. These findings were consistent with earlier research showing that adding oil improved the hydrophobic properties of the films (Hashemi & Khaneghah, 2017; Liu et al., 2021; Teymoorian et al., 2024). The contact angle of the present films was lower than that of native LDPE films (98.6°), as reported in a previous study (Aktas et al., 2023).

4. Conclusion

The current study successfully demonstrated the incorporation of MEO into collagen/k-carrageenan films as a promising approach for developing active packaging solutions. The anti-oxidant assays (DPPH and ABTS) confirmed that higher MEO concentrations improved the radical scavenging capacities of the films. Additionally, the anti-microbial properties were notably effective against *P. aeruginosa* and *C. albicans*, highlighting the potential of the films for active packaging. Overall, the study underscores the potential developed films as active packaging, offering improved anti-microbial and anti-oxidant properties. Increasing MEO concentrations led to a reduction in tensile strength and swelling index, which may restrict their use in applications requiring high mechanical integrity. Additionally, the films' moisture content decreased, potentially affecting their performance in high-humidity environments. While the films demonstrated enhanced anti-microbial and antioxidant properties, further optimization of MEO concentration is needed to balance functional performance with mechanical properties.

CRediT authorship contribution statement

Saurabh Bhatia: Writing – review & editing, Writing – original draft, Project administration, Conceptualization. **Muhammad Jawad:** Writing – original draft, Software, Methodology, Conceptualization. **Sampath Chinnam:** Writing – review & editing, Validation, Formal analysis, Data curation. **Ahmed Al-Harrasi:** Supervision, Project administration. **Yasir Abbas Shah:** Writing – review & editing, Writing

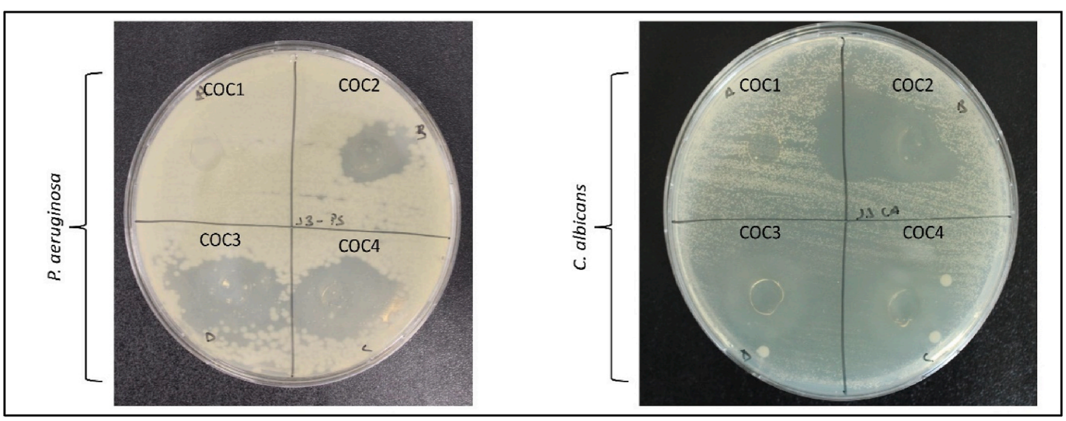

Fig. 7. The anti-microbial activity of blank and MEO incorporated COC films against *P. aeruginosa* and *C. albicans*. COC1 (control); COC2 (MEO 0.1 %); COC3 (MEO 0.5 %); COC4 (MEO 1 %).

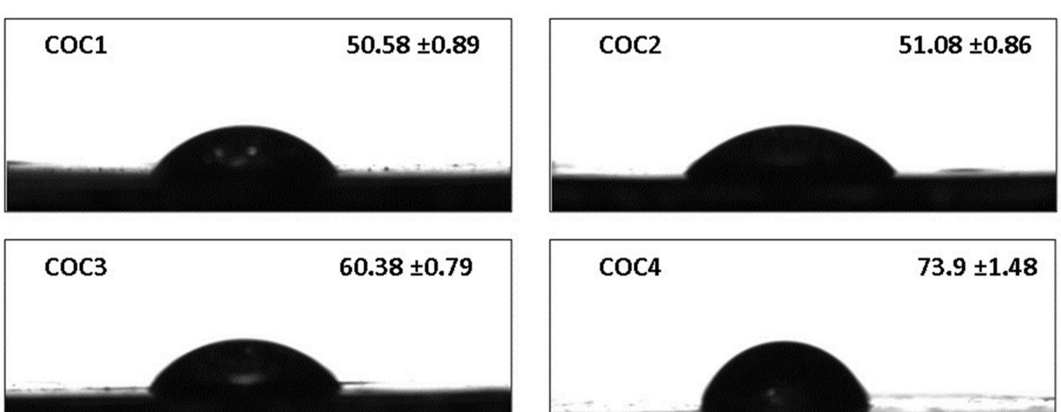

Fig. 8. The water contact angle of collagen + k-carrageenan films formulated with and without different concentrations of marjoram essential oil.

– original draft, Methodology. **Talha Shireen Khan:** Writing – review & editing, Software, Methodology. **Esra Koca:** Software, Methodology, Formal analysis, Data curation. **Levent Yurdaer Aydemir:** Writing – review & editing, Software, Data curation. **Sevgin Dıblan:** Writing – review & editing, Software, Methodology. **Dinu Thomas Thekkuden:** Validation, Resources, Formal analysis. **Fahad M. Alshabrmi:** Writing – review & editing, Validation, Formal analysis, Data curation. **Md Khalid Anwer:** Writing – review & editing, Formal analysis.

Funding

No Funding

Declaration of competing interest

Please find enclosed herewith the manuscript entitled "**Origanum majorana essential oil-enriched collagen/K-carrageenan films with enhanced thermal, hydrophobic, antioxidant and antimicrobial properties for active Packaging**" for publication in your esteemed journal. There is no conflict of interest among any of the authors whatsoever and all the authors have actively participated in the preparation of manuscript.

Acknowledgments

The Authors are thankful to the Natural and Medical Sciences Research Center, University of Nizwa, Oman, for providing research facilities to conduct the current study.

Data availability

Data will be made available on request.

References

Adam, F., Jamaludin, J., Abu Bakar, S. H., Abdul Rasid, R., & Hassan, Z. (2020). Evaluation of hard capsule application from seaweed: Gum Arabic-Kappa carrageenan biocomposite films. *Cogent Engineering, 7*(1), Article 1765682.

Aktas, C., Polat, O., Beitollahpoor, M., Farzam, M., Pesika, N. S., & Sahiner, N. (2023). Force-based characterization of the wetting properties of LDPE surfaces treated with CF4 and H2 plasmas. *Polymers, 15*(9), 2132.

Andonegi, M., de la Caba, K., & Guerrero, P. (2020). Effect of citric acid on collagen sheets processed by compression. *Food Hydrocolloids, 100*, Article 105427.

Andonegi, M., Irastorza, A., Izeta, A., de la Caba, K., & Guerrero, P. (2020). Physicochemical and biological performance of aloe vera-incorporated native collagen films. *Pharmaceutics, 12*(12), 1173.

Arfat, Y. A., Benjakul, S., Prodpran, T., Sumpavapol, P., & Songtipya, P. (2014). Properties and antimicrobial activity of fish protein isolate/fish skin gelatin film containing basil leaf essential oil and zinc oxide nanoparticles. *Food Hydrocolloids, 41*, 265–273.

Arrieta, M. P., Peltzer, M. A., López, J., del Carmen Garrigós, M., Valente, A. J., & Jiménez, A. (2014). Functional properties of sodium and calcium caseinate antimicrobial active films containing carvacrol. *Journal of Food Engineering, 121*, 94–101.

Ata, O., Bakar, B., Turkoz, B. K., Kumcuoglu, S., Aydogdu, Y., Gumustas, B., Doganay, G. D., Basturk, E., & Tavman, S. (2024). Structural and molecular characterization of collagen-type I extracted from lamb feet. *Journal of food science, 89*(1), 330–341.

Atef, M., Rezaei, M., & Behrooz, R. (2015). Characterization of physical, mechanical, and antibacterial properties of agar-cellulose bionanocomposite films incorporated with savory essential oil. *Food Hydrocolloids, 45*, 150–157.

Aziz, S. G.-G., & Almasi, H. (2018). Physical characteristics, release properties, and antioxidant and antimicrobial activities of whey protein isolate films incorporated with thyme (Thymus vulgaris L.) extract-loaded nanoliposomes. *Food and Bioprocess Technology, 11*, 1552–1565.

Aziz, M. S. A., Salama, H. E., & Sabaa, M. W. (2018). Biobased alginate/castor oil edible films for active food packaging. *LWT, 96*, 455–460.

Azizi, S., Mohamad, R., Rahim, R. A., Mohammadinejad, R., & Ariff, A. B. (2017). Hydrogel beads bio-nanocomposite based on Kappa-Carrageenan and green synthesized silver nanoparticles for biomedical applications. *International Journal of Biological Macromolecules, 104*, 423–431.

Bhatia, S., Abbas Shah, Y., Al-Harrasi, A., Jawad, M., Koca, E., & Aydemir, L. Y. (2024). Enhancing tensile strength, thermal stability, and antioxidant characteristics of transparent kappa carrageenan films using grapefruit essential oil for food packaging applications. *ACS Omega*.

Bhatia, S., Al-Harrasi, A., Jawad, M., Shah, Y. A., Al-Azri, M. S., Ullah, S., Anwer, M. K., Aldawsari, M. F., Koca, E., & Aydemir, L. Y. (2023). A comparative study of the properties of gelatin (porcine and bovine)-based edible films loaded with spearmint essential oil. *Biomimetics, 8*(2), 172.

Bonilla, J., Atarés, L., Vargas, M., & Chiralt, A. (2012). Effect of essential oils and homogenization conditions on properties of chitosan-based films. *Food Hydrocolloids, 26*(1), 9–16.

Brand-Williams, W., Cuvelier, M., & Berset, C. (1995). Antioxidative activity of phenolic composition of commercial extracts of sage and rosemary. *Lwt, 28*, 25–30.

Çakmak, H., Özselek, Y., Turan, O. Y., Fıratlıgil, E., & Karbancioğlu-Güler, F. (2020). Whey protein isolate edible films incorporated with essential oils: Antimicrobial activity and barrier properties. *Polymer Degradation and Stability, 179*, Article 109285.

Carbone, M., Donia, D. T., Sabbatella, G., & Antiochia, R. (2016). Silver nanoparticles in polymeric matrices for fresh food packaging. *Journal of King Saud University Science, 28*(4), 273–279.

Carneiro-da-Cunha, M. G., Cerqueira, M. A., Souza, B. W., Souza, M. P., Teixeira, J. A., & Vicente, A. A. (2009). Physical properties of edible coatings and films made with a polysaccharide from Anacardium occidentale L. *Journal of Food Engineering, 95*(3), 379–385.

Cimanga, K., Kambu, K., Tona, L., Apers, S., De Bruyne, T., Hermans, N., Totté, J., Pieters, L., & Vlietinck, A. J. (2002). Correlation between chemical composition and antibacterial activity of essential oils of some aromatic medicinal plants growing in the Democratic Republic of Congo. *Journal of Ethnopharmacology, 79*(2), 213–220.

Dashipour, A., Razavilar, V., Hosseini, H., Shojaee-Aliabadi, S., German, J. B., Ghanati, K., Khakpour, M., & Khaksar, R. (2015). Antioxidant and antimicrobial carboxymethyl cellulose films containing Zataria multiflora essential oil. *International Journal of Biological Macromolecules, 72*, 606–613.

Dong, Z., Xu, F., Ahmed, I., Li, Z., & Lin, H. (2018). Characterization and preservation performance of active polyethylene films containing rosemary and cinnamon essential oils for Pacific white shrimp packaging. *Food Control, 92*, 37–46.

El-Mesallamy, A. M., El-Gerby, M., Azim, M. H. A. E., & Awad, A. (2012). Antioxidant, antimicrobial activities and volatile constituents of clove flower buds oil. *Journal of essential oil bearing plants, 15*(6), 900–907.

Erdem, B. G., Dıblan, S., & Kaya, S. (2019). Development and structural assessment of whey protein isolate/sunflower seed oil biocomposite film. *Food and Bioproducts Processing, 118*, 270–280.

Gahruie, H. H., Ziaee, E., Eskandari, M. H., & Hosseini, S. M. H. (2017). Characterization of basil seed gum-based edible films incorporated with Zataria multiflora essential oil nanoemulsion. *Carbohydrate polymers, 166*, 93–103.

Ghani, S., Barzegar, H., Noshad, M., & Hojjati, M. (2018). The preparation, characterization and in vitro application evaluation of soluble soybean polysaccharide films incorporated with cinnamon essential oil nanoemulsions. *International Journal of Biological Macromolecules, 112*, 197–202.

Ghasemlou, M., Aliheidari, N., Fahmi, R., Shojaee-Aliabadi, S., Keshavarz, B., Cran, M. J., & Khaksar, R. (2013). Physical, mechanical and barrier properties of corn starch films incorporated with plant essential oils. *Carbohydrate polymers, 98*(1), 1117–1126.

Gheribi, R., Puchot, L., Verge, P., Jaoued-Grayaa, N., Mezni, M., Habibi, Y., & Khwaldia, K. (2018). Development of plasticized edible films from opuntia ficus-indica mucilage: A comparative study of various polyol plasticizers. *Carbohydrate polymers, 190*, 204–211.

Giraud-Guille, M.-M., Besseau, L., Chopin, C., Durand, P., & Herbage, D. (2000). Structural aspects of fish skin collagen which forms ordered arrays via liquid crystalline states. *Biomaterials, 21*(9), 899–906.

Haghighatpanah, N., Omar-Aziz, M., Gharaghani, M., Khodaiyan, F., Hosseini, S. S., & Kennedy, J. F. (2022). Effect of mung bean protein isolate/pullulan films containing marjoram (Origanum majorana L.) essential oil on chemical and microbial properties of minced beef meat. *International Journal of Biological Macromolecules, 201*, 318–329.

Hashemi, S. M. B., & Khaneghah, A. M. (2017). Characterization of novel basil-seed gum active edible films and coatings containing oregano essential oil. *Progress in Organic Coatings, 110*, 35–41.

Hasheminya, S.-M., Mokarram, R. R., Ghanbarzadeh, B., Hamishekar, H., Kafil, H. S., & Dehghannya, J. (2019). Development and characterization of biocomposite films made from kefiran, carboxymethyl cellulose and Satureja Khuzestanica essential oil. *Food Chemistry, 289*, 443–452.

Hopkins, E. J., Chang, C., Lam, R. S., & Nickerson, M. T. (2015). Effects of flaxseed oil concentration on the performance of a soy protein isolate-based emulsion-type film. *Food Research International, 67*, 418–425.

Jahed, E., Khaledabad, M. A., Bari, M. R., & Almasi, H. (2017). Effect of cellulose and lignocellulose nanofibers on the properties of Origanum vulgare ssp. gracile essential oil-loaded chitosan films. *Reactive and Functional Polymers, 117*, 70–80.

Jouki, M., Yazdi, F. T., Mortazavi, S. A., & Koocheki, A. (2014). Quince seed mucilage films incorporated with oregano essential oil: Physical, thermal, barrier, antioxidant and antibacterial properties. *Food Hydrocolloids, 36*, 9–19.

Kahya, N., Kestir, S. M., Öztürk, S., Yolaç, A., Torlak, E., Kalaycıoğlu, Z., Akın-Evingür, G., & Erim, F. B. (2022). Antioxidant and antimicrobial chitosan films enriched with aqueous sage and rosemary extracts as food coating materials: Characterization of the films and detection of rosmarinic acid release. *International Journal of Biological Macromolecules, 217*, 470–480.

Kang, J.-H., & Song, K. B. (2019). Characterization of Job's tears (Coix lachryma-jobi L.) starch films incorporated with clove bud essential oil and their antioxidant effects on pork belly during storage. *LWT, 111*, 711–718.

Kavoosi, G., Rahmatollahi, A., Dadfar, S. M. M., & Purfard, A. M. (2014). Effects of essential oil on the water binding capacity, physico-mechanical properties,

antioxidant and antibacterial activity of gelatin films. *LWT-Food Science and Technology, 57*(2), 556–561.
Kchaou, H., Jridi, M., Benbettaieb, N., Debeaufort, F., & Nasri, M. (2020). Bioactive films based on cuttlefish (Sepia officinalis) skin gelatin incorporated with cuttlefish protein hydrolysates: Physicochemical characterization and antioxidant properties. *Food Packaging and Shelf Life, 24*, Article 100477.
Kim, J. O., Park, J. K., Kim, J. H., Jin, S. G., Yong, C. S., Li, D. X., Choi, J. Y., Woo, J. S., Yoo, B. K., & Lyoo, W. S. (2008). Development of polyvinyl alcohol–sodium alginate gel-matrix-based wound dressing system containing nitrofurazone. *International journal of pharmaceutics, 359*(1–2), 79–86.
Lee, J. Y., Garcia, C. V., Shin, G. H., & Kim, J. T. (2019). Antibacterial and antioxidant properties of hydroxypropyl methylcellulose-based active composite films incorporating oregano essential oil nanoemulsions. *LWT, 106*, 164–171.
Lei, Y., Mao, L., Yao, J., & Zhu, H. (2021). Improved mechanical, antibacterial and UV barrier properties of catechol-functionalized chitosan/polyvinyl alcohol biodegradable composites for active food packaging. *Carbohydrate polymers, 264*, Article 117997.
Liu, Z., Lin, D., Shen, R., Zhang, R., Liu, L., & Yang, X. (2021). Konjac glucomannan-based edible films loaded with thyme essential oil: Physical properties and antioxidant-antibacterial activities. *Food Packaging and Shelf Life, 29*, Article 100700.
Martins, J. T., Cerqueira, M. A., Bourbon, A. I., Pinheiro, A. C., Souza, B. W., & Vicente, A. A. (2012). Synergistic effects between κ-carrageenan and locust bean gum on physicochemical properties of edible films made thereof. *Food Hydrocolloids, 29*(2), 280–289.
Matuschek, E., Brown, D. F., & Kahlmeter, G. (2014). Development of the EUCAST disk diffusion antimicrobial susceptibility testing method and its implementation in routine microbiology laboratories. *Clinical Microbiology and Infection, 20*(4), O255–O266.
Mehanna, S., Issa, M. Y., Hassan, N. H., Hussien, A. M., Ibrahim, M. A., & Hassanen, E. I. (2022). Origanum majorana essential oil improves the rat's sexual behavior and testicular oxidative damage induced by imidacloprid via modulating the steroidogenesis pathways. *Saudi Pharmaceutical Journal, 30*(9), 1315–1326.
Moni, S. S., Hadi Sultan, M., Makeen, H. A., Jabeen, A., Sanobar, S., Siddiqui, R., ur Rehman, Z., Alam, M. S., Ahmad, S., & Elmobark, M. E. (2021). Phytochemical and spectral analysis of the methanolic extracts of leaves of Murraya koenigii of Jazan, Saudi Arabia. *Natural Product Research, 35*(15), 2569–2573.
Najafian, L. (2023). A review of bioactive peptides as functional food ingredients: Mechanisms of action and their applications in active packaging and food quality improvement. *Food & Function, 14*(13), 5835–5857.
Ortiz-Tafoya, M., & Tecante, A. (2018). Physicochemical characterization of sodium stearoyl lactylate (SSL), polyoxyethylene sorbitan monolaurate (Tween 20) and κ-carrageenan. *Data in Brief, 19*, 642–650.
Park, H. J. (1996). Gas and mechanical barrier properties of carrageenan-based biopolymer films. *식품과학과 산업, 29*(2), 47–53.
Paudel, P. N., Satyal, P., Satyal, R., Setzer, W. N., & Gyawali, R. (2022). Chemical composition, enantiomeric distribution, antimicrobial and antioxidant activities of Origanum majorana L. essential oil from Nepal. *Molecules, 27*(18), 6136.
Prasetyaningrum, A., Utomo, D. P., Raemas, A. F. A., Kusworo, T. D., Jos, B., & Djaeni, M. (2021). Alginate/κ-carrageenan-based edible films incorporated with clove essential oil: Physico-chemical characterization and antioxidant-antimicrobial activity. *Polymers, 13*(3), 354.
Raut, S., Raut, S., Sharma, M., Srivastav, C., Adhikari, B., & Sen, S. K. (2015). Enhancing degradation of low density polyethylene films by Curvularia lunata SG1 using particle swarm optimization strategy. *Indian Journal of Microbiology, 55*, 258–268.
Re, R., Pellegrini, N., Proteggente, A., Pannala, A., Yang, M., & Rice-Evans, C. (1999). Antioxidant activity applying an improved ABTS radical cation decolorization assay. *Free radical biology and medicine, 26*(9–10), 1231–1237.
Rezaei, A., Aligholi, H., Zeraatpisheh, Z., Gholami, A., & Mirzaei, E. (2021). Collagen/chitosan-functionalized graphene oxide hydrogel provide a 3D matrix for neural stem/precursor cells survival, adhesion, infiltration and migration. *Journal of Bioactive and Compatible Polymers, 36*(4), 296–313.
Sakdapipanich, J., Rodgerd, P., & Sakdapipanich, N. (2022). A low-density polyethylene (LDPE)/Macca carbon advanced composite film with functional properties for packaging materials. *Polymers, 14*(9), 1794.
Salama, H. E., Aziz, M. S. A., & Sabaa, M. W. (2019). Development of antibacterial carboxymethyl cellulose/chitosan biguanidine hydrochloride edible films activated with frankincense essential oil. *International Journal of Biological Macromolecules, 139*, 1162–1167.
Sani, I. K., Pirsa, S., & Tağı, Ş. (2019). Preparation of chitosan/zinc oxide/Melissa officinalis essential oil nano-composite film and evaluation of physical, mechanical and antimicrobial properties by response surface method. *Polymer Testing, 79*, Article 106004.
Schmidt, E., Bail, S., Buchbauer, G., Stoilova, I., Krastanov, A., Stoyanova, A., & Jirovetz, L. (2008). Chemical composition, olfactory evaluation and antioxidant effects of the essential oil of Origanum majorana L. from Albania. *Natural Product Communications, 3*(7), Article 1934578X0800300704.
Seol, K.-H., Lim, D.-G., Jang, A., Jo, C., & Lee, M. (2009). Antimicrobial effect of κ-carrageenan-based edible film containing ovotransferrin in fresh chicken breast stored at 5 C. *Meat Science, 83*(3), 479–483.
Shen, Z., & Kamdem, D. P. (2015). Development and characterization of biodegradable chitosan films containing two essential oils. *International Journal of Biological Macromolecules, 74*, 289–296.
Shojaee-Aliabadi, S., Hosseini, H., Mohammadifar, M. A., Mohammadi, A., Ghasemlou, M., Hosseini, S. M., & Khaksar, R. (2014). Characterization of κ-carrageenan films incorporated plant essential oils with improved antimicrobial activity. *Carbohydrate polymers, 101*, 582–591.
Shojaee-Aliabadi, S., Hosseini, H., Mohammadifar, M. A., Mohammadi, A., Ghasemlou, M., Ojagh, S. M., Hosseini, S. M., & Khaksar, R. (2013). Characterization of antioxidant-antimicrobial κ-carrageenan films containing Satureja hortensis essential oil. *International Journal of Biological Macromolecules, 52*, 116–124.
Simona, J., Dani, D., Petr, S., Marcela, N., Jakub, T., & Bohuslava, T. (2021). Edible films from carrageenan/orange essential oil/trehalose—structure, optical properties, and antimicrobial activity. *Polymers, 13*(3), 332.
Simsek, M., Eke, B., & Demir, H. (2020). Characterization of carboxymethyl cellulose-based antimicrobial films incorporated with plant essential oils. *International Journal of Biological Macromolecules, 163*, 2172–2179.
Song, X., Zuo, G., & Chen, F. (2018). Effect of essential oil and surfactant on the physical and antimicrobial properties of corn and wheat starch films. *International Journal of Biological Macromolecules, 107*, 1302–1309.
Soni, A., Kandeepan, G., Mendiratta, S., Shukla, V., & Kumar, A. (2016). Development and characterization of essential oils incorporated carrageenan based edible film for packaging of chicken patties. *Nutrition & Food Science, 46*(1), 82–95.
Soysal, Ç., Bozkurt, H., Dirican, E., Güçlü, M., Bozhüyük, E. D., Uslu, A. E., & Kaya, S. (2015). Effect of antimicrobial packaging on physicochemical and microbial quality of chicken drumsticks. *Food Control, 54*, 294–299.
Sun, H., Li, S., Chen, S., Wang, C., Liu, D., & Li, X. (2020). Antibacterial and antioxidant activities of sodium starch octenylsuccinate-based Pickering emulsion films incorporated with cinnamon essential oil. *International Journal of Biological Macromolecules, 159*, 696–703.
Testing, A. S.f. (2002). *Materials, Standard test method for tensile properties of thin plastic sheeting*. Astm International.
Teymoorian, M., Moghimi, R., Hosseinzadeh, R., Zandi, F., & Lakouraj, M. M. (2024). Fabrication the emulsion-based edible film containing Dracocephalum kotschyi Boiss essential oil using chitosan–gelatin composite for grape preservation. *Carbohydrate Polymer Technologies and Applications, 7*, Article 100444.
Tongnuanchan, P., Benjakul, S., & Prodpran, T. (2013). Physico-chemical properties, morphology and antioxidant activity of film from fish skin gelatin incorporated with root essential oils. *Journal of Food Engineering, 117*(3), 350–360.
Tongnuanchan, P., Benjakul, S., & Prodpran, T. (2014). Comparative studies on properties and antioxidative activity of fish skin gelatin films incorporated with essential oils from various sources. *International Aquatic Research, 6*, 1–12.
Udo, T., Mummaleti, G., Mohan, A., Singh, R. K., & Kong, F. (2023). Current and emerging applications of carrageenan in the food industry. *Food Research International*, Article 113369.
Vedhanayagam, M., Anandasadagopan, S., Nair, B. U., & Sreeram, K. J. (2020). Polymethyl methacrylate (PMMA) grafted collagen scaffold reinforced by PdO–TiO2 nanocomposites. *Materials Science and Engineering: C, 108*, Article 110378.
Wang, Z., Hu, S., & Wang, H. (2017). Scale-up preparation and characterization of collagen/sodium alginate blend films. *Journal of Food Quality, 2017*.
Xue, F., Gu, Y., Wang, Y., Li, C., & Adhikari, B. (2019). Encapsulation of essential oil in emulsion based edible films prepared by soy protein isolate-gum acacia conjugates. *Food Hydrocolloids, 96*, 178–189.
Yahaya, M. F., Kubmarawa, D., Yelwa, J. M., & Runde, M. (2018). Antioxidant and antimicrobial activity of essential oils extracted from aromatic plants. *World Scientific News, 111*, 13–25.
Yasar, S., Nizamlıoglu, N. M., Gucus, M. O., Bildik Dal, A. E., & Akgul, K.b. (2022). Origanum majorana L. essential oil-coated paper acts as an antimicrobial and antioxidant agent against meat spoilage. *ACS Omega, 7*(10), 9033–9043.
Yekta, R., Mirmoghtadaie, L., Hosseini, H., Norouzbeigi, S., Hosseini, S. M., & Shojaee-Aliabadi, S. (2020). Development and characterization of a novel edible film based on Althaea rosea flower gum: Investigating the reinforcing effects of bacterial nanocrystalline cellulose. *International Journal of Biological Macromolecules, 158*, 327–337.
Zhang, L., Liu, Z., Sun, Y., Wang, X., & Li, L. (2020). Effect of α-tocopherol antioxidant on rheological and physicochemical properties of chitosan/zein edible films. *Lwt, 118*, Article 108799.
Zhou, Y., Wu, X., Chen, J., & He, J. (2021). Effects of cinnamon essential oil on the physical, mechanical, structural and thermal properties of cassava starch-based edible films. *International Journal of Biological Macromolecules, 184*, 574–583.